Supporting information

Programmable Locomotion Mechanisms of Nanowires with Semi-Hard Magnetic Properties Near a Surface Boundary

Bumjin Jang,[†] Ayoung Hong,[†] Carlos Alcantara,[†] George Chatzipirpiridis,[†] Xavier Martí,[¶] Eva Pellicer, [‡] Jordi Sort, [‡,§] , Yuval Harduf,[⊥] Yizhar Or,*,[⊥] Bradley J. Nelson,*,[†] and Salvador Pané*,[†]

†Institute of Robotics and Intelligent Systems, ETH Zurich, Zurich, CH-8092, Switzerland

¶ Institute of Physics, Academy of Sciences of the Czech Republic, Cukrovarnická 10, 162 00 Praha 6, Czech Republic

‡ Departament de Física, Universitat Autònoma de Barcelona, E-08193 Bellaterra, Spain

§ Institució Catalana de Recerca i Estudis Avançats (ICREA), Pg. Lluís Companys 23, E-08010 Barcelona, Spain

⊥ Faculty of Mechanical Engineering, Technion Israel Institute of Technology, Haifa, 3200003, Israel

Corresponding Authors

*E-mail: vidalp@ethz.ch

E-mail: bnelson@ethz.ch

E-mail: izi@me.technion.ac.il

Supporting figures and tables

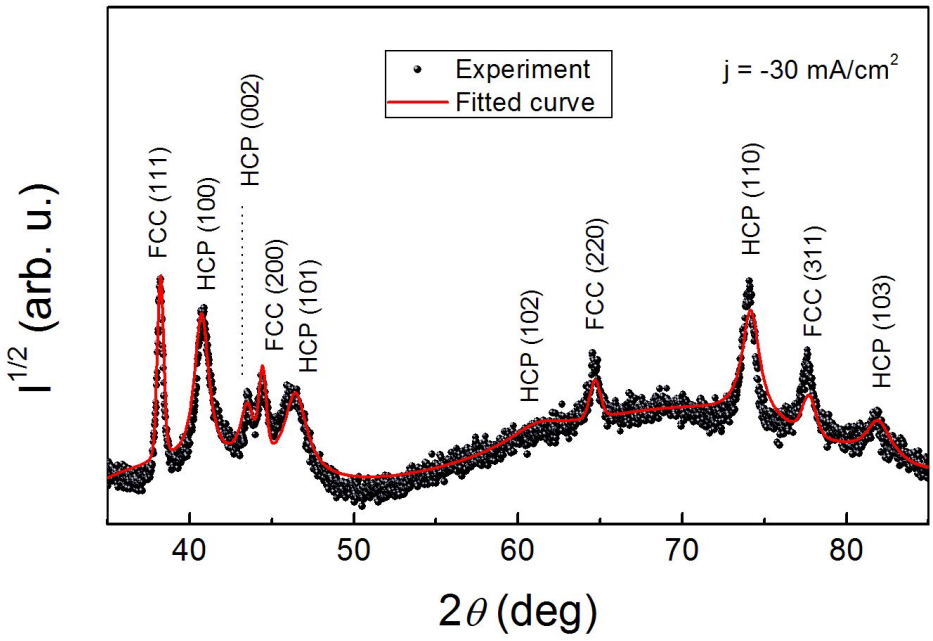

Figure S1: Experimental XRD pattern of the CoPt nanowires grown at j = -30 mA/cm^2. The red line corresponds to a full-pattern refinement of the experimental pattern using the Rietveld method and taking crystallographic texture and the occurrence of stacking faults into account.

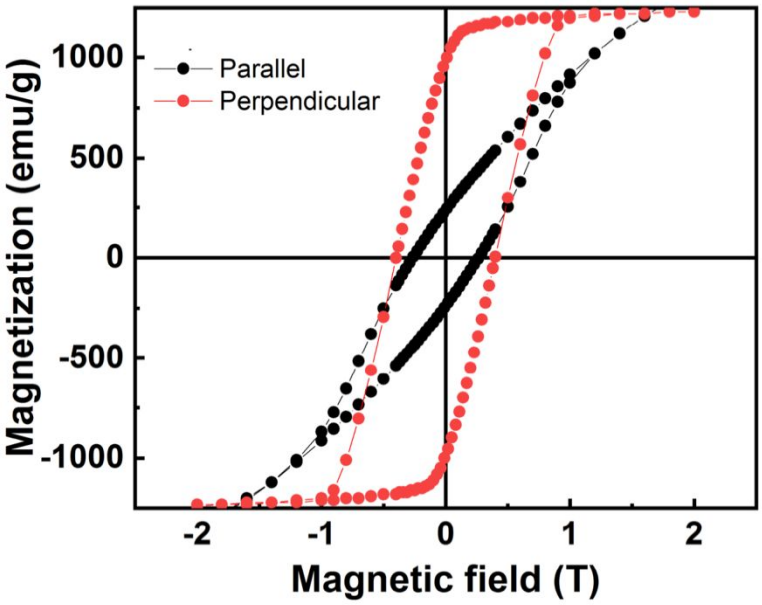

Figure S2. Magnetization curves (emu/cm^3) of the synthesized CoPt nanowires.

Hydrodynamic resistance of the body moving near the wall

Yang *et al.*[1] have discussed the hydrodynamic drag force acting on the object near the boundary when it translates or rotates. As described in the main text, the applied drag force is described as

$$\boldsymbol{F}^{e}_{drag} = \boldsymbol{K}_T\boldsymbol{U}^e + \boldsymbol{K}_C^T\boldsymbol{\Omega}^e$$

with the resistance tensor $\boldsymbol{K}_T, \boldsymbol{K_C}$. Each component of the matrix is a function of the body tilt angle θ, the distance of the body center from the surface d, the dynamic viscosity of a liquid η, and the body slenderness $\epsilon = \ln\left(\frac{2l}{R}\right)^{-1}$ as follow:

$$K_T^{11} = -4\pi\eta l(\sin\theta^2 + 1)\epsilon\left[1 - \epsilon\left(\ln 2 - 1 + \frac{3\sin^2\theta - 1}{2(1+\sin^2\theta)} + \frac{1}{4l}\int_{-l}^{l} A(x)dx\right)\right] + O(\epsilon^3)$$

$$K_T^{13} = 2\pi\eta l\sin 2\theta\epsilon\left[1 - \epsilon\left(\ln 2 + \frac{1}{2} + \frac{1}{4l}\int_{-l}^{l} D(x)dx\right)\right] + O(\epsilon^3)$$

$$K_T^{22} = -8\pi\eta l\epsilon\left[1 - \epsilon\left(\ln 2 - \frac{1}{2} + \frac{1}{4l}\int_{-l}^{l} B(x)dx\right)\right] + O(\epsilon^3)$$

$$K_T^{31} = 2\pi\eta l\sin 2\theta\epsilon\left[1 - \epsilon\left(\ln 2 + \frac{1}{2} + \frac{1}{4l}\int_{-l}^{l} E(x)dx\right)\right] + O(\epsilon^3)$$

$$K_T^{33} = -4\pi\eta l(\cos\theta^2 + 1)\epsilon\left[1 - \epsilon\left(\ln 2 - 1 + \frac{3\cos^2\theta - 1}{2(1+\cos^2\theta)} + \frac{1}{4l}\int_{-l}^{l} C(x)dx\right)\right] + O(\epsilon^3)$$

$$K_C^{12} = 2\pi\eta\sin\theta\epsilon^2\int_{-l}^{l} xH(x)dx + O(\epsilon^3)$$

$$K_C^{21} = -2\pi\eta\sin\theta\epsilon^2\int_{-l}^{l} xB(x)dx + O(\epsilon^3)$$

$$K_C^{23} = -2\pi\eta\cos\theta\epsilon^2\int_{-l}^{l} xJ(x)dx + O(\epsilon^3)$$

$$K_C^{32} = 2\pi\eta\cos\theta\epsilon^2 \int_{-l}^{l} xB(x)dx + O(\epsilon^3)$$

The specific formulae for $A(x)$, $B(x)$, $C(x)$, $D(x)$,$E(x)$, $H(x)$, and $J(x)$ can be found in the Appendix of Yang *et al.*[1]

Simulation with external force (gravitational and buoyant forces)

Once the gravitational and buoyant forces in Z-direction are considered, the nanowire gets closer to the wall as the simulation runs. Therefore, over three periods the total hydrodynamic forces on the body increase in every direction, which causes a slight increase on the speed of the translational motion.

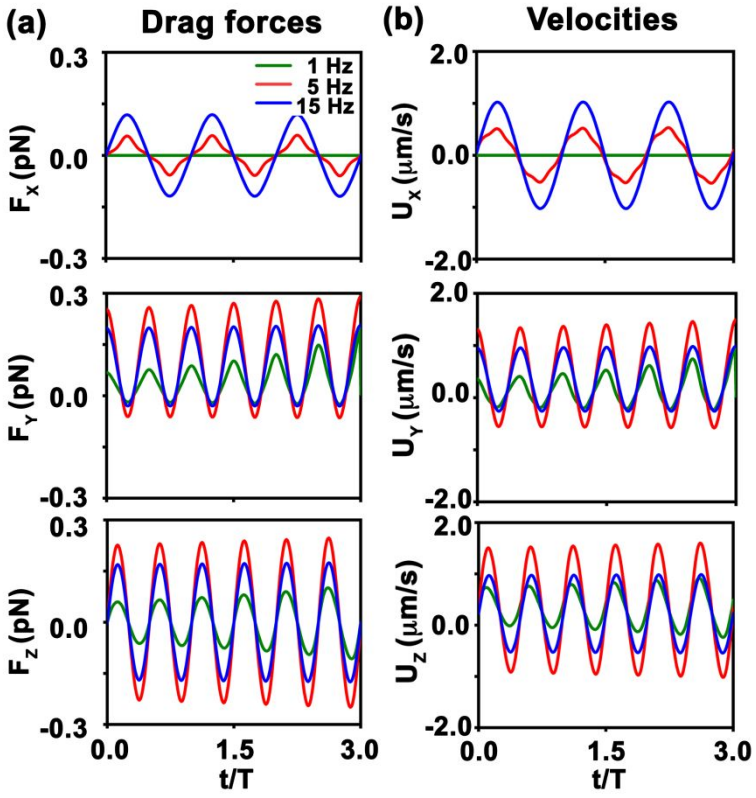

Figure S3. Simulated (a) drag forces and (b) velocities taking into account the external forces (gravitational and buoyant forces).

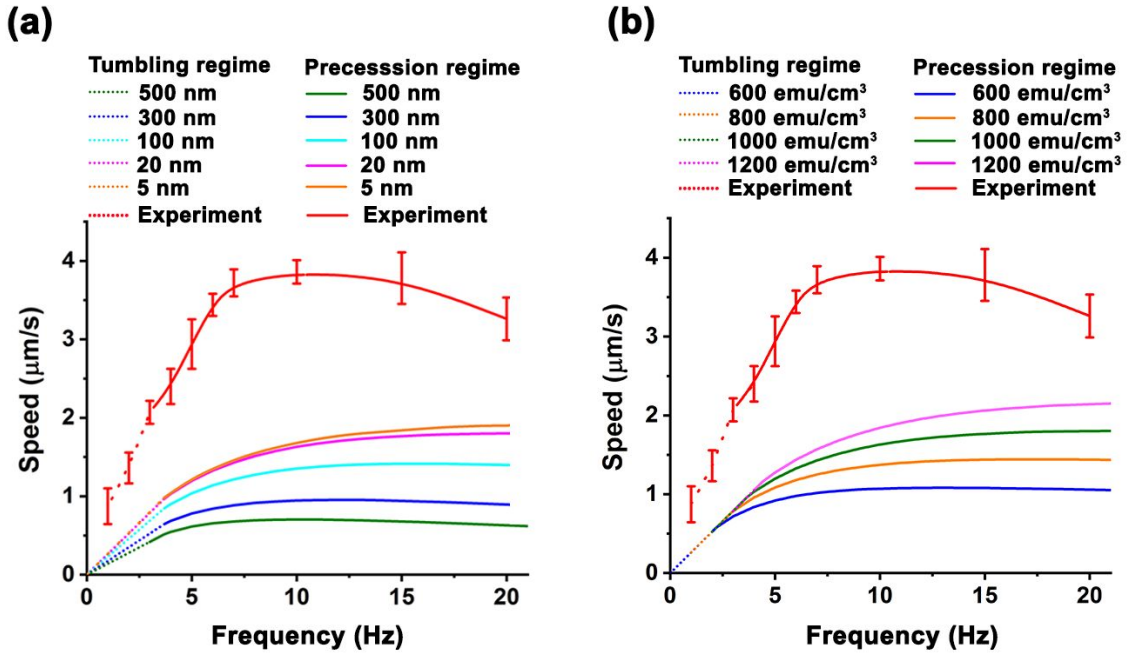

Figure S4. The effects of (a) distance from the wall and (b) the magnitude of magnetic moment ($\vec{m}$) on the speed of CoPt nanowires. Simulation (a) was conducted at different initial tip distances (5, 20, 100, 300, and 500 nm) at $\vec{m}$ = 1000 emu/cm^3. Simulation (b) was conducted at an initial tip distances of 20 nm.

Table S1. Summary of the crystallographic information obtained from Rietveld refinements of the XRD patterns.

Co HCP solid solution	*a* cell parameter (nm)	0.2561
	c cell parameter (nm)	0.4162
	Crystallite size (nm)	14.5
	Microstrains	8×10^{-5}
	Stacking fault probability	0.0492
Pt FCC solid solution	*a* cell parameter (nm)	0.4085
	Crystallite size (nm)	96.0
	Microstrains	0.0037
	Stacking fault probability	N/A

Table S2. Coercivities and M/Ms values of CoPt nanowires in (a) perpendicular and (b) parallel to nanowire's axis, electrochemically deposited at -30 mA/cm^2

Coercivity (Oe) in perpendicular to the nanowire's long axis	2000	3200	4000
M_r/M_s in perpendicular to the nanowire's long axis	0.4006	0.6484	0.8154
Coercivity (Oe) in parallel to the nanowire's long axis	2300	2900	2600
M_r/M_s in parallel to the nanowire's long axis	0.2261	0.2429	0.1845

Supporting movies

Movie S1. The motion of CoNi nanowire (control sample) under a xy-planar rotating magnetic field (AVI).

Movie S2. The motion of CoPt nanowire under a xy-planar rotating magnetic field (AVI) (AVI).

Movie S3. Motion transformation of CoPt nanowire as increasing the frequency of a xz-planar rotating magnetic field (AVI).

Movie S4. A vortex formation around the tip of CoPt nanowire moving with precession motion (AVI).

Movie S5**.** A vortex formation at the center of CoPt nanowire moving with rolling motion (AVI).

References

1. Yang, S.-M.; Leal, L. G., "Particle Motion in Stokes Flow near a Plane Fluid-Fluid Interface. Part 1. Slender Body in a Quiescent Fluid. *J. Fluid Mech.* **2006,** *136*, 393-421.